[February, 1974] BULLETIN OF THE CHEMICAL SOCIETY OF JAPAN, VOL. 47(2), 249—256 (1974) 249

The Electrodepositions of Copper and Nickel from Their Trifluoroacetate-Formamide Baths

Tatsuko Takei

The Faculty of Engineering, Shinshu University, Wakasato, Nagano 380

(Received March 9, 1973)

The present author has been studying the electrodeposition of metals from non-aqueous solutions of metal trifluoroacetates. In the present study, the properties of the $Cu(CF_3COO)_2$–$HCONH_2$ bath and the $Ni(CF_3COO)_2$–$HCONH_2$ bath, and the mechanism of the electrodeposition of copper and nickel from these baths, were studied. Both $Cu(CF_3COO)_2$ and $Ni(CF_3COO)_2$ were easily dissolved in formamide. The specific conductance of these solutions was high. Satisfactory electrodeposits are obtained from these solutions, with a high current efficiency. The cross-section of the electrodeposits showed a granular structure. The rate of the electrodeposition of copper from the $Cu(CF_3COO)_2$–$HCONH_2$ bath and that of nickel from the $Ni(CF_3COO)_2$–$HCONH_2$ bath were controlled by the charge-transfer reaction at low current densities. The activation overvoltage of the hydrogen-evolution reaction for the electrolysis of the CF_3COOH–$HCONH_2$ bath was higher than that for the electrolysis of the CF_3COOH–H_2O bath.

Menzies *et al.*[1] and Brenner[2,3] pointed out the importance of the study of the electrodeposition of metals from non-aqueous solutions. Studies[2–5] have already been made of various metals.

However, none has thus far been used industrially. In the deposition of metals from non-aqueous solutions, it is hard to find metal salts that are readily soluble in an organic solvent or a solvent which forms a complex ion in a suitable strength with metal ions in the solutions. Moreover, little is known about the properties of the solutions and the mechanism of the electrodeposition of metals.

The present author has been studying the electrodeposition of metals from non-aqueous solvents by the use of metal salts of trifluoroacetic acid. In the present study, examinations were made into the nature of the $Cu(CF_3COO)_2$–$HCONH_2$ bath and that of the $Ni(CF_3COO)_2$–$HCONH_2$ bath, which dissolve $Cu(CF_3COO)_2$ or $Ni(CF_3COO)_2$ respectively, using formamide. Formamide has a high boiling point and a high dielectric constant and readily forms complex ions with metal ions. Electrodeposition was performed in these baths in order to examine the effect of the condition of electrolysis on the current efficiency and on the electrodeposit. The overvoltages were measured by the interrupter method in order to analyze the electrodeposition reactions. Measurements were also made on the hydrogen overvoltage in the formamide bath.

The deposition of copper from the $Cu(CF_3COO)_2$–$HCONH_2$ bath was compared with that of nickel from the $Ni(CF_3COO)_2$–$HCONH_2$ bath.

Experimental

Reagent. *Formamide*: For the measurement of the conductance, the solubility, and the viscosity, guaranteed reagent-grade formamide containing about 0.02% moisture was used. For the electrodeposition and the measurement of the overvoltage, commercial first-grade reagent formamide containing about 0.12% moisture was used.

$Cu(CF_3COO)_2$ and $Ni(CF_3COO)_2$: These substances were prepared by the neutralization method from copper hydroxide and nickel hydroxide with trifluoroacetic acid. The purities of the corresponding products were 99.4 and 99.8% respectively.

Other Chemicals: Phosphoric acid and acetic acid of the first-grade reagent were used. Sulfuric-, nitric-, and hydrochloric acids of a special grade were used.

Measurement of the Solubility. The solubility of $Cu(CF_3COO)_2$ in formamide was measured by the gravimetric determination of copper in a definite amount of a saturated solution obtained by dissolving $Cu(CF_3COO)_2$ in formamide at 20 °C. The gravimetric determination of copper was done by the use of oxine.

Measurement of the Conductance. The electrolytic conductance of $Cu(CF_3COO)_2$–$HCONH_2$ and $Ni(CF_3COO)_2$–$HCONH_2$ solutions was determined by the use of a Yanagimoto electrolytic conductometer MY-7. Before the measurement the solutions to be measured were kept for about an hour at 30, 40, and 50 °C in a thermostat.

Viscosity Measurement. The viscosity of the $Ni(CF_3COO)_2$–$HCONH_2$ solutions was measured by means of an Ostwald viscosimeter at 30.0±0.1 °C.

Density Measurement. The densities of the formamide and $Ni(CF_3COO)_2$–$HCONH_2$ solutions were determined by the use of a Springel densimeter at 30.0±0.1 °C.

Electrodeposition. The electrodeposition was performed by the use of the apparatus shown in Fig. 1. In the case of

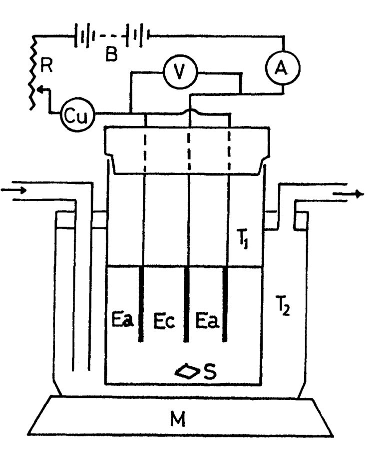

Fig. 1. Apparatus for metal plating.
A: Ammeter, B: Battery, Cu: Copper coulometer, Ea: anode, Ec: cathode, M: Magnetic stirrer, R: Slide rheostat, S: Stirrer, T_1: Electrolysis cell, T_2: Thermostat, V: Voltmeter, W: Water (const. temp.)

copper electrodeposition, two copper plates and one iron plate were used as anode and cathode respectively. For nickel deposition, two nickel plates and one copper plate were used as anode and cathode respectively. These electrodes were pretreated by the usual method as indicated.[6] Nitrogen was passed through formamide for about 30 minutes. A definite amount of the $Cu(CF_3COO)_2$ or $Ni(CF_3COO)_2$ was dissolved in the formamide solution to give a bath used for the electrodeposition. The bath was stirred at a definite rate. The electrodeposition was carried out at a current density of 0.5—15.0 A/dm^2 at 30—70 °C.

The thickness of the electrodeposited layer was about 5 μ, the thickness being calculated from the amount electricity used for the deposition.

Observation of the Electrodeposited Surface and the Electrodeposited Layer. For these observations, a metallurgical microscope was used.

The specimen with an electrodeposited layer, about 30 μ thick, was mounted in resin and etched.

Analysis of Gases and Electrolytic Solutions. During the electrolysis, a slight evolution of gases from the cathode and the anode was noticed. Therefore, the gases and the electrolytic solution were analyzed by gas-chromatography in order to examine the composition of the gases and the mechanism of the reaction. For the measurement, a gas-chromatograph, Type GCG-220, made by the Yanagimoto Manufacturing Co., Ltd, was used. The packing materials of the column were silicon DC 550 at 53 °C and 100 °C, and active carbon at 33 °C, used for the analysis of the electrolytic solution and of the gas respectively.

Measurement of the Overvoltage. The overvoltage of the copper electrodeposition was measured at 30, 40, and 50 °C for the baths containing 100, 200, and 400 g $Cu(CF_3COO)_2$ per liter respectively. The overvoltage of nickel deposition was measured at 50, 60, and 70 °C for the baths containing 50, 100, 150 g $Ni(CF_3COO)_2$ per liter respectively. The measuement was made by the current-interrupter method, with stirring at a definite rate.

The measurement of the overvoltage of hydrogen evolution was made by the same method as above at 50 °C, in a 0.1 N CF_3COOH–H_2O bath and also in a 0.1 N CF_3COOH–$HCONH_2$ bath.

A platinized-platinum electrode (length, 3 mm; diameter, 0.3 mm) was used as a reference electrode for the measurement of the overvoltage.

A current-interrupter, Type CI-2515, made by the Hokuto Electric Works Co., Ltd., was used.

Results and Discussion

The Properties of Formamide Solutions. *Solvolysis*: According to Röhler, solvolysis takes place in formamide solutions of copper sulfate and nickel chloride.[7] Therefore, solvolysis can be expected to take place in formamide solutions of $Cu(CF_3COO)_2$ and $Ni(CF_3COO)_2$ by means of the following reaction:

$$M(CF_3COO)_2 + 4HCONH_2 \rightarrow M(HCONH)_2\cdot 2HCONH_2 + 2CF_3COOH \quad (1)$$

where M represents copper or nickel.

Actually, a light yellow-green precipitate is formed in the $Ni(CF_3COO)_2$–$HCONH_2$ solution by the reaction of $Ni(CF_3COO)_2$ with formamide. This reaction becomes more remarkable with a rise in the bath temperature and with an increase in the $Ni(CF_3COO)_2$ concentration.

When the reaction product was filtered, an almost colorless filtrate was obtained. The gas-chromatographic analysis of this solution showed the presence of CF_3COOH. The precipitate was washed, dried, and then gravimetrically analyzed with dimethyl glyoxime in order to determine the nickel content in the precipitate. The nickel content was about 96.8% of the theoretical amount of Ni in $Ni(HCONH)_2\cdot 2HCONH_2$. It was found by these results that the reaction shown in Eq. (1) takes place in the $Ni(CF_3COO)_2$–$HCONH_2$ solution.

CF_3COOH was also detected in the $Cu(CF_3COO)_2$–$HCONH_2$ solution. Therefore, it is likely that the reaction shown by Eq. (1) also takes place in this bath.

Solubility. At 20 °C, 182 g $Cu(CF_3COO)_2$ was dissolved in 100 g of formamide. Consequently, the solubility of $Cu(CF_3COO)_2$ in formamide is larger than those in methanol and acetonitrile[8]. The solvolysis takes place very easily in a formamide solution with a high concentration of $Ni(CF_3COO)_2$. Therefore, the solubility of $Ni(CF_3COO)_2$ in formamide could not be determined.

Specific Conductance. Figure 2 shows the specific conductance of the $Cu(CF_3COO)_2$–$HCONH_2$ solution. The specific conductance of the $Cu(CF_3COO)_2$–$HCONH_2$ solution was almost the same as that of the $Ni(CF_3COO)_2$–$HCONH_2$ solution and about 1.5 times that of the $Cu(CF_3COO)_2$–MeOH solution.[8]

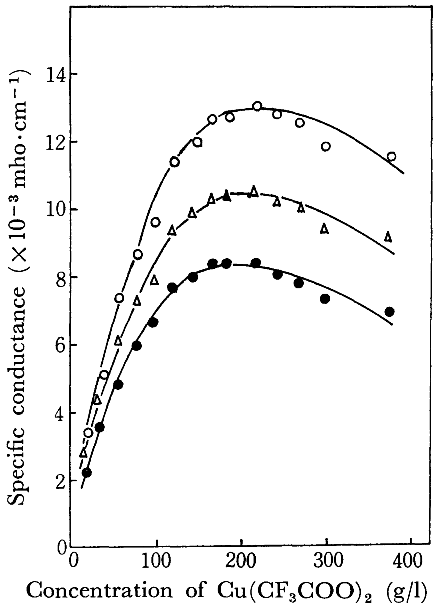

Fig. 2. Specific conductance of $Cu(CF_3COO)_2$–$HCONH_2$ solutions.
-●-: 30 °C, -△-: 40°C, -○-: 50°C

The specific conductance approached a definite value when the $Cu(CF_3COO)_2$ concentration reached about 200 g/l at any temperature. In the solutions containing more than 200 g of $Cu(CF_3COO)_2$, copper trifluoroacetate does not seem to dissociate any more; on the contrary, it seems that the movement of ions in the solutions is interfered with by the presence of non-dissociated salts.

Viscosity. The viscosity of the $Ni(CF_3COO)_2$–

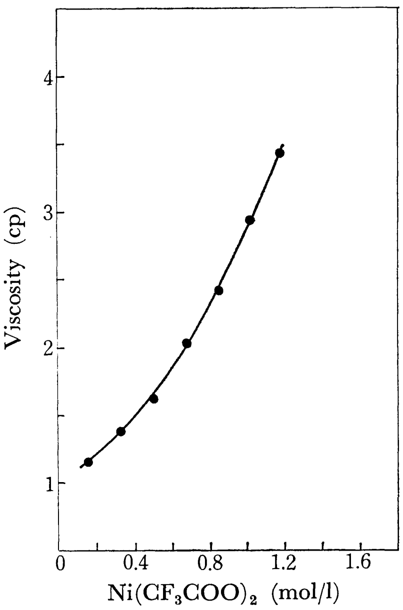

Fig. 3. Relationship between viscosity and concentration of Ni(CF$_3$COO)$_2$ in Ni(CF$_3$COO)$_2$-HCONH$_2$ solutions at 30°C.

HCONH$_2$ solution as a function of the concentration of Ni(CF$_3$COO)$_2$ is shown in Fig. 3. It may be seen in Fig. 3 that the viscosity increases almost linearly with the increase in the Ni(CF$_3$COO)$_2$ concentration. It thus appears that the viscosity of the Cu(CF$_3$COO)$_2$–HCONH$_2$ solution increases with the increase in the Cu(CF$_3$COO)$_2$ concentration, like that of the Ni(CF$_3$COO)$_2$–HCONH$_2$ solution.

Electrodeposition. *Copper Electrodeposition*: Figure 4 shows an example of the current density-current efficiency curve of copper deposition from the Cu(CF$_3$COO)$_2$–HCONH$_2$ bath.

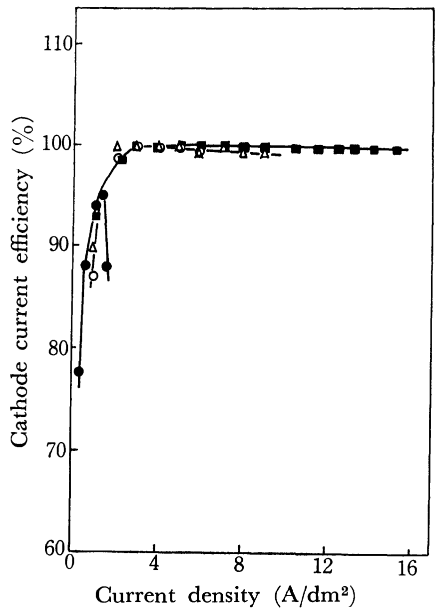

Fig. 4—1. Cathode current efficiency as a function of current density at 40°C.

-●-: Cu(CF$_3$COO)$_2$ 20 g/HCONH$_2$ 1 l
-○-: Cu(CF$_3$COO)$_2$ 100 g/HCONH$_2$ 1 l
-△-: Cu(CF$_3$COO)$_2$ 200 g/HCONH$_2$ 1 l
-■-: Cu(CF$_3$COO)$_2$ 400 g/HCONH$_2$ 1 l

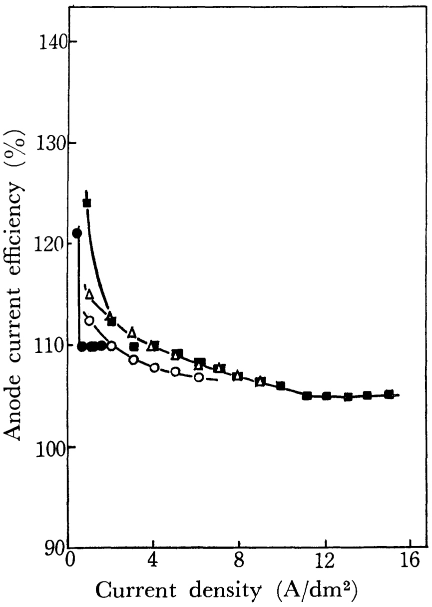

Fig. 4—2. Anode current efficiency as a function of current density at 40 °C.

-●-: Cu(CF$_3$COO)$_2$ 20 g/HCONH$_2$ 1 l
-○-: Cu(CF$_3$COO)$_2$ 100 g/HCONH$_2$ 1 l
-△-: Cu(CF$_3$COO)$_2$ 200 g/HCONH$_2$ 1 l
-■-: Cu(CF$_3$COO)$_2$ 400 g/HCONH$_2$ 1 l

The cathodic current efficiency was close to 100% irrespective of the Cu(CF$_3$COO)$_2$ concentration. However, the efficiency tends to decrease with the rise in the bath temperature.

It was noticed that a very small amount of hydrogen gas evolved from the cathode during the electrolysis. The lowering of the cathodic current efficiency is attributable to this evolution of hydrogen gas. The evolution of hydrogen gas is attributable to the discharge of hydrogen ions formed by the dissociation of CF$_3$COOH, which was itself derived from the reaction shown in Eq. (1).

On the other hand, the anodic current efficiency was found to be more than 100% irrespective of the concentration of Cu(CF$_3$COO)$_2$ and of the bath temperature. The efficiency even exceeded 110% at a low current density. This efficiency is attributable to the chemical reaction of copper with the CF$_3$COOH formed by the reaction given by Eq. (1).

No gases evolved from the anode.

Figure 5 shows the current density region in which bright and smooth deposits are obtained. At any temperature, bright and smooth deposits were observed over a wide range of current density when the concentration of Cu(CF$_3$COO)$_2$ was high.

From the results mentioned above, it was confirmed that bright and smooth deposits of copper are obtained with a high efficiency over a wide region of current density from the Cu(CF$_3$COO)$_2$ 400 g/l–HCONH$_2$ bath at 40 °C.

Electrodeposition of Nickel: An example of the current density-current efficiency curve for the nickel deposition from Ni(CF$_3$COO)$_2$–HCONH$_2$ bath is shown

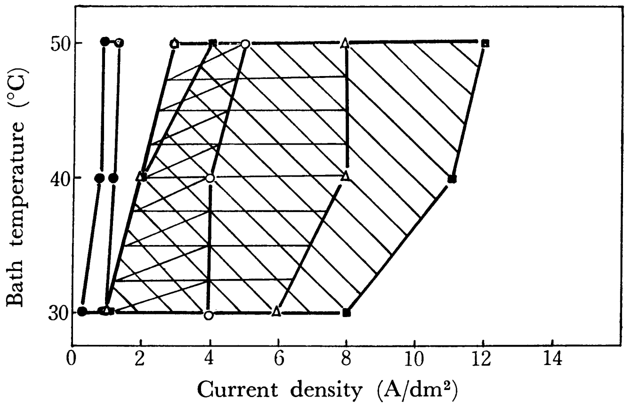

Fig. 5. The range of current density for bright and smooth copper deposit.
●: $Cu(CF_3COO)_2$ 20 g/$HCONH_2$ 1 l
○: $Cu(CF_3COO)_2$ 100 g/$HCONH_2$ 1 l
△: $Cu(CF_3COO)_2$ 200 g/$HCONH_2$ 1 l
■: $Cu(CF_3COO)_2$ 400 g/$HCONH_2$ 1 l

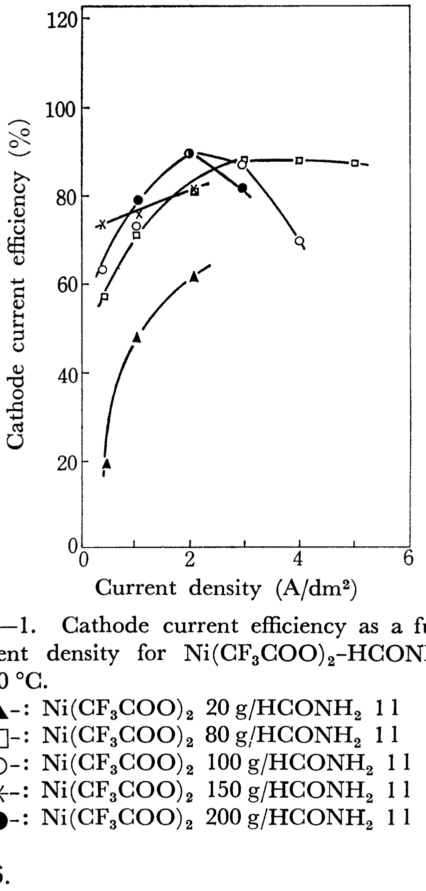

Fig. 6—1. Cathode current efficiency as a function of current density for $Ni(CF_3COO)_2$-$HCONH_2$ baths at 50 °C.
-▲-: $Ni(CF_3COO)_2$ 20 g/$HCONH_2$ 1 l
-□-: $Ni(CF_3COO)_2$ 80 g/$HCONH_2$ 1 l
-○-: $Ni(CF_3COO)_2$ 100 g/$HCONH_2$ 1 l
-✕-: $Ni(CF_3COO)_2$ 150 g/$HCONH_2$ 1 l
-●-: $Ni(CF_3COO)_2$ 200 g/$HCONH_2$ 1 l

in Fig. 6.

With the increase in the $Ni(CF_3COO)_2$ concentration, the cathodic current efficiency increased, but the anodic current efficiency tended to decrease.

When the $Ni(CF_3COO)_2$ concentration was 80—100 g/l, the anodic current efficiency was close to 100% irrespective of the bath temperature. However, the cathodic current efficiency was low at 50 °C and 70 °C when the current density was high. Only at 60 °C was the efficiency about 90% at a high current density.

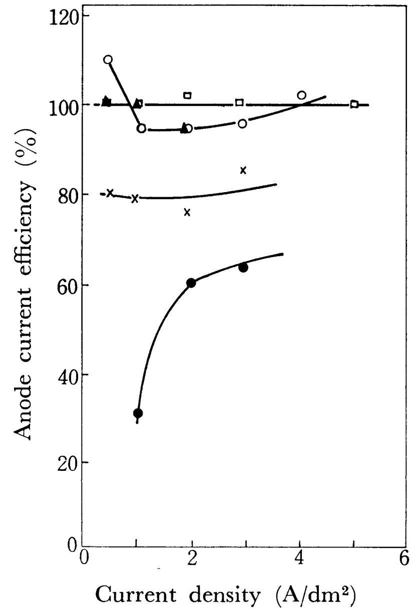

Current density (A/dm²)

Fig. 6—2. Anode current efficiency as a function of current density for $Ni(CF_3COO)_2$-$HCONH_2$ baths at 50 °C.
-▲-: $Ni(CF_3COO)_2$ 20 g/$HCONH_2$ 1 l
-□-: $Ni(CF_3COO)_2$ 80 g/$HCONH_2$ 1 l
-○-: $Ni(CF_3COO)_2$ 100 g/$HCONH_2$ 1 l
-✕-: $Ni(CF_3COO)_2$ 150 g/$HCONH_2$ 1 l
-●-: $Ni(CF_3COO)_2$ 200 g/$HCONH_2$ 1 l

The discharge of the H^+ formed by the dissociation of CF_3COOH in the bath occurred on the cathode during the electrolysis in the $Ni(CF_3COO)_2$–$HCONH_2$ bath, as in the case of the $Cu(CF_3COO)_2$–$HCONH_2$ bath, resulting in the evolution of a small amount of hydrogen. From the $Ni(CF_3COO)_2$–$HCONH_2$ bath, the evolution of carbon dioxide gas occurred from the anode. However, the amount of carbon dioxide evolved was much smaller than that of the gas evolved from the cathode.

The deposits from the $Ni(CF_3COO)_2$–$HCONH_2$ bath were easily peeled off from the substrate when the $Ni(CF_3COO)_2$ concentration or the bath temperature was low. Table 1 shows the current-density region in which a lustrous and adherent nickel deposit is obtained.

From the results mentioned above, it was confirmed that the conditions which give a lustrous and adherent deposit from the $Ni(CF_3COO)_2$–$HCONH_2$ bath with a high efficiency are: $Ni(CF_3COO)_2$ concentration,

Table 1. The range of current density for bright and adherent nickel deposit in $Ni(CF_3COO)_2$-$HCONH_2$ bath
(unit of current density : A/dm²)

Bath temp. (°C)	$Ni(CF_3COO)_2$ (g/l)			
	80	100	150	200
40	1.0—2.0		0.5—1.0	
50	1.0—2.0	1.0—2.0	0.5—2.0	1.0—2.0
60		0.5—2.0		
70		0.5—4.0		

80—100 g/l; bath temperature, 60 °C; and current density, 0.5—2.0 A/dm^2.

It will be possible to widen the current-density region which gives satisfactory deposits if the adherence of the deposits to the substrate is improved by the addition of an appropriate additive to the Ni-$(CF_3COO)_2$–$HCONH_2$ bath.

Appearance on Deposited Surface and the Structure of the Deposited Layer. An example of the deposited surface and the deposited layer of nickel and copper is shown in Photograph 1. The deposited surfaces of copper and nickel are very smooth and consist of very fine grains when the deposition has been made at a low current density. The grains on the electrodeposited surface of nickel were especially fine. With the increase in the current density, all the deposits tended to show round blocks and cracks.

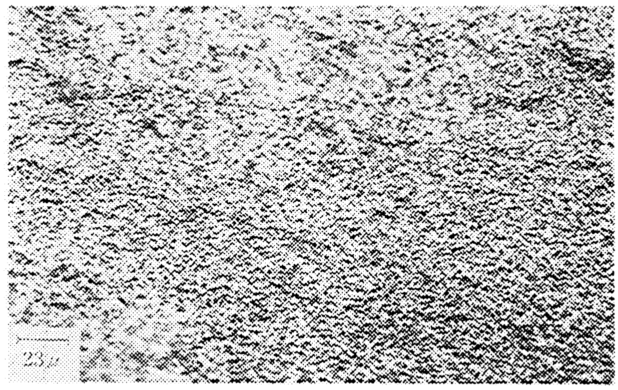

Photo. 1—1. Surface of copper deposit obtained from $Cu(CF_3COO)_2$ (400 g)/$HCONH_2$ (1 l) bath at 11.0 A/dm^2 at 50 °C.

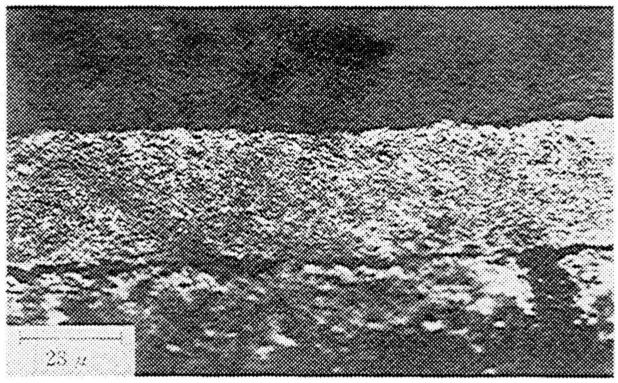

Photo. 1—2. Cross-section of copper deposit obtained from $Cu(CF_3COO)_2$ (400 g)/$HCONH_2$ (1 l) bath at 4.0 A/dm^2 at 30 °C.

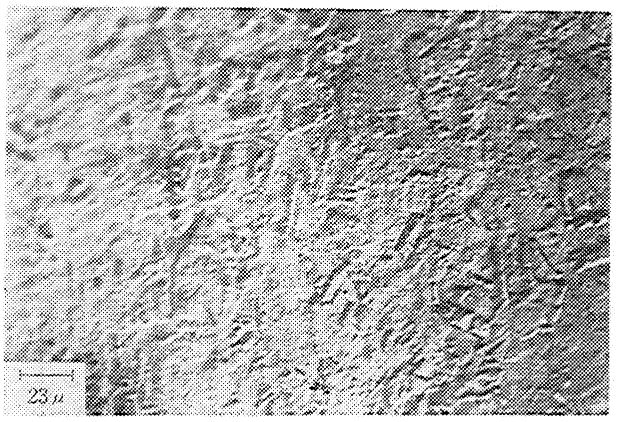

Photo. 1—3. Surface of nickel deposit obtained from $Ni(CF_3COO)_2$ (100 g)/$HCONH_2$ (1 l) bath at 1.0 A/dm^2 at 60 °C.

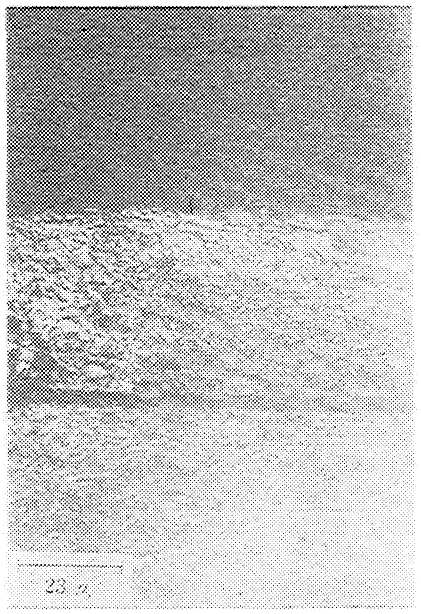

Photo. 1—4. Cross-section of nickel deposit obtained from $Ni(CF_3COO)_2$ (100 g)/$HCONH_2$ (1 l) bath at 1.0 A/dm^2 at 50 °C.

It was possible to obtain dense deposits when the bath temperature was high.

The structures of the deposits of copper and nickel were granular. The copper- and nickel- ions in the $HCONH_2$ baths form complex ions. The ligands which are adsorbed on the electrode during electrodeposition, suppress any surface diffusion of the adatom and prevent the growth of the nucleus in the vertical direction. Therefore, the frequency of the nucleus formation increases. It appears that the fine grains are produced to form a granular structure.

Activation Overvoltage. From the decay curve of the overvoltage 4 ms after the interruption of the electrolytic current, the resistance polarization was subtracted. The remainder was assumed to be the activation overvoltage.

The Relation between the Current Density (i_c) and the Activation Overvoltage (η_c) of the Electrodeposition of Copper or Nickel: The electrodeposition of metals from the solvated metal complex ions is [11] generally complicated.

This experiment was based upon the thought that the charge-transfer reaction is rate-determining within the range of current density (*i.e.* the Tafel region) with a straight-line relation between the current density and the activation overvoltage. According to the present experiment, the Tafel region was found to be in the range of current density, of 0.7—1.5 A/dm^2 at a bath temperature of 30 °C, in that of 0.8—2.0 A/dm^2 at 40 °C, and in that of 0.9—3.5 A/dm^2 at 50 °C for copper deposition. The ranges of the current density were 0.9—2.3 A/dm^2 at 50 °C, 0.9—4.4 A/dm^2 at 60 °C, and 0.9—4.8 A/dm^2 at 70 °C for nickel

Table 2. Parameters of the deposition reaction of copper from $Cu(CF_3COO)_2$-$HCONH_2$ bath

Concn. of $Cu(CF_3COO)_2$ (mol/l) × 10^{-2}	Bath temp. (°C)	i_{oc} (A/dm²)	α_c	$\alpha_c n$	n	b_c (−V)
35	30	0.44	0.717	0.503	0.704	0.120
	40	0.56	0.773	0.558	0.721	0.112
	50	0.64	0.838	0.765	0.913	0.084
70	30	0.54	0.717	0.524	0.734	0.105
	40	0.63	0.773	0.623	0.806	0.100
	50	0.72	0.838	0.804	0.959	0.080
140	30	0.64	0.717	0.446	0.625	0.135
	40	0.74	0.773	0.578	0.748	0.108
	50	0.80	0.838	0.620	0.741	0.104

Table 3. Parameters of the deposition reaction of nickel from $Ni(CF_3COO)_2$-$HCONH_2$ bath

Concn. of $Ni(CF_3COO)_2$ (mol/l) × 10^{-2}	Bath temp. (°C)	i_{oc} (A/dm²)	α_c	$\alpha_c n$	n	b_c (−V)
17.5	50	0.030	0.520	0.644	1.23	0.100
	60	0.055	0.694	0.604	0.870	0.110
	70	0.070	0.764	0.684	0.895	0.100
35.0	50	0.040	0.520	0.602	1.15	0.107
	60	0.065	0.694	0.651	0.938	0.102
	70	0.080	0.764	0.735	0.962	0.093
52.5	50	0.050	0.520	0.607	1.16	0.106
	60	0.075	0.694	0.651	0.938	0.102
	70	0.090	0.764	0.684	0.895	0.100

deposition.

The Apparent Exchange Current Density (i_{oc}) of the Copper and Nickel Depositions: The apparent exchange current density of copper and nickel depositions was obtained by extrapolating the η_c in the relation of η_c—i_c to 0. The apparent exchange current density was thus determined at various temperatures and various salt concentrations. The results are shown in Tables 2 and 3.

The values of the i_{oc} of the copper and nickel depositions tended to increase with the salt concentration in the bath and with the bath temperature.

It was noticed that the i_{oc} of the nickel deposition was smaller than that of the copper deposition.

The Apparent Transfer Coefficient (α_c) and the Apparent Valence (n) of Copper and Nickel Depositions: On the Tafel curves, Eqs. (2) and (3) hold among n, α_c, i_{oc}, the apparent standard rate constant (K_{SR}), and the concentration of Cu^{2+} or Ni^{2+}, C_0 mol/l:

$$i_c = i_{oc}\exp(-\alpha_c Fn\eta_c/RT) \tag{2}$$

$$i_{oc} = nFK_{SR}C_0^{(1-\alpha_c)} \tag{3}$$

If the plot of log i_{oc}—log C_0 becomes linear in Eq. (3), its slope is equal to $(1-\alpha_c)$. This relation is shown in Fig. 7 for the deposition of copper from the $Cu(CF_3COO)_2$–$HCONH_2$ bath as an example. Similar results were obtained for the deposition of nickel from the $Ni(CF_3COO)_2$–$HCONH_2$ bath. The relation was approximately linear. Therefore, α_c was determined from the slope. On the other hand, the slopes of the Tafel line are equal to $2.303\times RT/\alpha_c nF$ as is given by Eq. (2). Therefore, $\alpha_c n$ was determined from this relationship. Tables 2 and 3 show α_c, $\alpha_c n$, n and the slopes of the Tafel lines.

As an average of these results, the following relations were found for copper deposition;

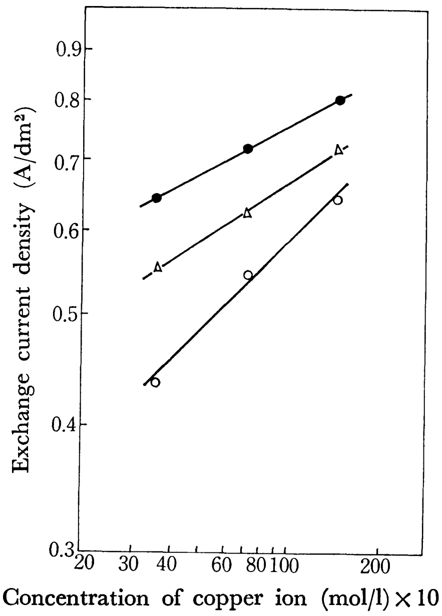

Fig. 7. Relationship between exchange current density and concentration of copper ion.
-○-: 30 °C, -△-: 40 °C, -●-: 50 °C

$\alpha_c = 0.78$ (namely, dlog i_{oc}/dlog $C_0=0.22$)

$n = 0.77$

The slope of the Tafel line $(b_c) = -0.113$ V. For nickel deposition:

$\alpha_c = 0.66$ (namely, dlog i_{oc}/dlog $C_0 = 0.34$)

$n = 1.00$

$b_c = -0.102$ V.

Therefore, it may be concluded that the reaction proceeds as is shown in Eqs. (4) and (5) within the range of 0.7—3.5 A/dm^2 for copper deposition from the $Cu(CF_3COO)_2$–$HCONH_2$ bath and within that of 0.9—4.8 A/dm^2 for nickel deposition from the $Ni(CF_3COO)_2$–$HCONH_2$ bath.

$$M^{2+} + e^- \rightarrow M^+ \quad (4)$$

$$M^+ + e^- \rightarrow M \quad (5)$$

where M is Cu or Ni.

It may also be concluded that the reaction of Eq. (4) is rate-determining, because the effect of the potential (current density) on the electrodeposition is relatively slight at low current densities, which give satisfactory deposits.

It seems that the solvation[11] has some effect on the deposition of metals.

The Apparent Activation Energy of Copper and Nickel Depositions: The relation between i_{oc} and the bath temperature (T) is given by the Arrhenius equation. Thus,

$$i_{oc} = K \exp(-E_c/RT) \quad (6)$$

where E_c: the apparent activation energy of the deposition of metals. K: a constant.

Figure 8 shows the relation between the apparent exchange current density and the bath temperature (namely, $\log i_{oc} - 1/T$) for the copper deposition. This relation is approximately shown by a straight line. The same relation also holds for the nickel deposition. The apparent activation energies of the deposition of copper and nickel were determined from the slopes of these curves.

It was thus found that the apparent activation energies were 3.50 kcal/mol, 2.86 kcal/mol, and 2.46 kcal/mol for the deposition of copper from the baths containing 100, 200, and 400 g $Cu(CF_3COO)_2$ per liter respectively. For the deposition of nickel, the activation energies were 8.85 kcal/mol, 8.03 kcal/mol, and 6.31 kcal/mol for the baths containing 50, 100, 150 g $Ni(CF_3COO)_2$ per liter respectively.

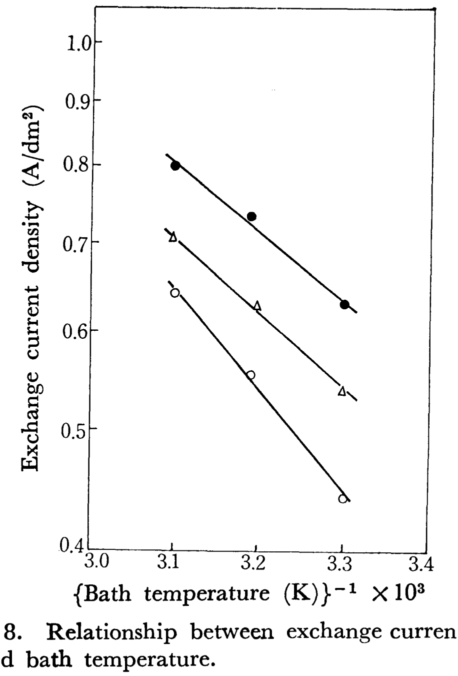

Fig. 8. Relationship between exchange current density and bath temperature.

-●-: concentration of copper ion 140×10^{-2} mol/l
-△-: concentration of copper ion 70×10^{-2} mol/l
-○-: concentration of copper ion 35×10^{-2} mol/l

That is, the activation energy of the copper deposition from the $Cu(CF_3COO)_2$–$HCONH_2$ bath was 2.9 kcal/mol on the average, while that of the nickel deposition from the $Ni(CF_3COO)_2$–$HCONH_2$ bath was 7.7 kcal/mol on the average. In the high-concentration solutions of $Cu(CF_3COO)_2$ or $Ni(CF_3COO)_2$, the true concentration of Cu^{2+} or Ni^{2+} is lower than that of $Cu(CF_3COO)_2$ or $Ni(CF_3COO)_2$. Therefore, it is likely that the true activation energy is larger than those values.

The activation energy of the direct deposition of Cu^{2+} from a copper borofluoride bath is estimated to be about 11—12 kcal/mol.[9] The activation energy as determined by the present study is lower than this value. It may be concluded, in view of the activation energy, that the deposition of copper from the $Cu(CF_3COO)_2$–$HCONH_2$ bath takes place through Cu^+ and that the deposition of nickel takes place through Ni^+.

The Electrodeposition of Metals from a Metal Trifluoroacetate-$HCONH_2$ Bath. It is not sufficient to discuss the deposition of metals from a metal trifluoroacetate–$HCONH_2$ bath from the viewpoint of copper deposition and nickel deposition only. However, the following tendencies were noticed:

(1) Formamide well dissolves metal trifluoroacetate. In this solution, metal-complex ions are formed.

(2) The i_{oc} value of the deposition of metals from a formamide bath is larger than that from an aqueous solution. However, the metals which show large i_{oc} values in aqueous solutions also show large i_{oc} values in formamide baths. Those which show small i_{oc} values in aqueous solutions also show small i_{oc} values in formamide baths.

(3) When the i_{oc} values are large, metals are easily deposited and the deposits are apt to be coarse.[10] In formamide baths, a metal-complex are formed. Therefore, the growth in the perpendicular direction is suppressed, resulting in an increase in the frequency of nucleation. Therefore, a smooth deposited surface with small crystallites is obtained.

(4) In the formamide bath, the i_{oc} values of metal deposition are larger than in aqueous baths. The values of i_{oc} vary little with the kind of metal. It is, therefore, possible to accelerate the deposition of metals, which are hardly deposited at all from aqueous solutions.

Activation Overvoltage of Hydrogen Evolution. When the electrolysis was performed in the CF_3COOH–$HCONH_2$ bath, hydrogen gas evolved from the cathode. However, no gases evolved from the anode.

The activation overvoltage of hydrogen evolution from the CF_3COOH–$HCONH_2$ bath is higher than that from an aqueous solution. Therefore, hardly any evolution of hydrogen takes place in formamide baths because of the activation overvoltage.

The author wishes to express her deep gratitude to Professor Rimpei Kojima for his kind direction and encouragement throughout this work.

References

1) I. A. Menzies, T. Broughton, and V. O. Nwoko, *Trans. Inst. Metal Finishing*, **43**, 9 (1965).

2) A. Brenner, "Advances in Electrochemistry and Electrochemical Engineering" ed. by P. Delahay and C. W. Tobias, Vol. 5, Interscience Pub. (1967) p. 206.

3) D. E. Couch and A. Brenner, *J. Electrochem. Soc.*, **99**, 234 (1952).

4) A. Brenner, *ibid.*, **103**, 652 (1956).

5) H. Connor and A. Brenner, *ibid.*, **103**, 657 (1956).

6) S. Yoshizawa, "Denkikagakuzikkenho", Izumi Shobō (1964), p. 108.

7) H. Röhler, *Z. Electrochem.*, **16**, 419 (1910).

8) T. Takei and R. Kojima, "Nipponkagakukai 19 nenkai Kōenyokōshu", 1ZB, 209 (1966); "Nipponkagakukai 20 nenkai Kōenyokōshu", II, 2C, 204 (1967).

9) Y. Ueno, M. Tsuiki, F. Hine, and S. Yoshizawa, *Denkikagaku*, **32**, 211 (1964).

10) T. Yoshida and N. Nomoto, *ibid.*, **34**, 600 (1966).

11) T. Hayashi, *Kinzokuhyomengijutsu*, **21**, 515 (1970).